

# Modeling and measurement of locking stability for a fiber Fabry–Pérot tunable filter based on the dithering technique

HAIBING QI<sup>1, 2</sup>, YONGLIN YU<sup>1\*</sup>, WEI CHEN<sup>1</sup>

<sup>1</sup>Wuhan National Laboratory for Optoelectronics, College of Optoelectronics Science and Engineering, Huazhong University of Science and Technology, Wuhan 430074, China

<sup>2</sup>School of Electric and Electronic Information Engineering, Huangshi Institute of Technology, Huangshi, 435003, China

\*Corresponding author: yonglinyu@mail.hust.edu.cn

An impulse response method and Fourier transformation are proposed to theoretically analyze the dynamic characteristics of a tunable FFP filter. And the dynamic optical spectrum and time domain characteristics of a FFP tunable filter modulated by an alternating current (AC) dithering signal are derived. The simulated and experimental results show that the method can determine the relation between the AC signal parameters and the dynamic response through either the output optical signal or the output electrical signal. Our experimental results also reveal the dependence of the locking stability of a FFP tunable filter on the amplitude of a dithering signal.

Keywords: fiber Fabry–Pérot tunable filter, impulse response method, dithering technique, locking stability.

## 1. Introduction

Fiber Fabry–Pérot (FFP) tunable filters are critical components in such applications as high-speed optical packet switching, phase-to-intensity modulation conversion and efficiency improvement in radio over fiber (RoF) links, and wavelength demodulating for sensors [1–3]. Narrower bandwidth piezoelectric transducer (PZT) driven tunable filters have the advantage of higher sensitivity, but they are easy to drift from the target wavelength. Therefore, precise and stable control of the tunable filters is required, especially for dynamic tracking and locking. The locking stability based on the dithering technique varies and depends on the characteristics of the FFP tunable filter and the dithering signal [4, 5]. Thus, it is highly desirable to predict dynamic behaviors of the filter with the dithering control for optimization design in the above-mentioned applications.

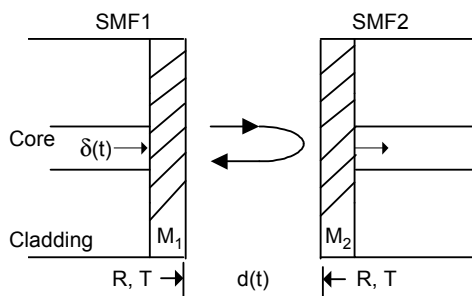
In the areas of frequency stabilization for a laser [6] and the measurement of characterization of a high finesse optical resonator [7, 8], the dynamic response of a fixed Fabry–Pérot (FP) cavity with a frequency-dithered laser [9] has been studied extensively. For the issue of the cavity length dithering, a phasor representation approach was introduced to derive the linear differential equation of the normalized length scan rate [10], and a transfer function transformed from the time domain dynamic field in the cavity was utilized to analyze the exact condition for resonance in a FP cavity [11]. The above studies provide the potential for analyzing the dynamic responses of a FFP tunable filter with the cavity length dithering. However, a few analytical methods have been reported in literature for predicting the relationship between the locking stability of a FFP tunable filter and the parameters of an alternating current (AC) dithering signal.

In this paper, a signal processing method is proposed to model the dynamic responses of a FFP tunable filter with the dithering control technique. We focus on predicting the relationship between the locking stability of a FFP tunable filter and the parameters of an AC dithering signal. Based on the static analysis of the FFP filter at the state of fixed cavity length, a dynamic frequency response was obtained by modifying the transfer function of the device for the case of cavity length modulated by a dithering signal. Effects of the amplitude and frequency of the AC dithering signal on locking stability can be observed from simulation results, either from the frequency responses or the time response. Experimental results also reveal the dependence of the locking stability of a FFP tunable filter on the amplitude of a dithering signal, which is in accordance with the numerical results.

## 2. Dynamic response of a FFP tunable filter

### 2.1. Frequency response at the state of fixed cavity length

In general, a FFP tunable filter consists of two closely spaced single mode fibers (SMFs) with an air gap between them, which can maintain high sensitivity with highly reflective mirrors ( $M_1$  and  $M_2$ ) coated on the parallel fiber end faces, as shown in Figure 1.  $R$  and  $T$  are the two mirrors' effective reflection and effective transmission, respectively,  $d(t)$  is the FP cavity length,  $\tau$  represents the time interval between



◀ Fig. 1. Structure of FFP tunable filter.

any adjacent beams at the output end of the mirror  $M_2$ , which is one round-trip time in the cavity and is given by

$$\tau = \frac{2d_0}{c} \quad (1)$$

where  $d_0$  is the cavity length at a certain bias voltage,  $c$  is the speed of light, and  $\tau = 1/\Omega_F$ , ( $\Omega_F$  is the free spectral range (FSR) when the cavity is fixed at the original length  $d_0$ ). When the incident beam is a single pulse  $\delta(t)$ , the impulse response function of the filter can be described by

$$h(t) = \sum_{n=0}^{\infty} a_n \delta(t - \tau_n) \quad (2)$$

where  $\delta(x)$  is the Dirac delta function,  $a_n = T(\eta R)n$ ,  $\tau_n = n\tau$ ,  $n$  is an integer,  $\eta$  is the efficiency factor determined by the insertion loss. The occurrence time of the first transmitted pulse is set at  $t = 0$ . Then the frequency response  $H(\omega)$  of the FFP filter can be calculated by Fourier transforms [12]

$$H(\omega) = \int_0^{\infty} h(t) \exp(-j\omega t) dt = \sum_{n=0}^{\infty} a_n \exp(-j\omega n \tau) \quad (3)$$

where  $\omega$  is the angular frequency of an incident single pulse. In the field of signal processing, the phase frequency characteristics  $\varphi(\omega)$  can be expressed as

$$\varphi(\omega) = -\tan^{-1} \left[ \frac{\text{Re}(H(\omega))}{\text{Im}(H(\omega))} \right] \quad (4)$$

With the dithering technique, the FP cavity modulated by an AC signal needs to maintain quasi-static resonance. Since the Fourier series  $H(\omega)$  is the infinite sum of delayed versions of the input signal weighted by the roundtrip cavity reflection, a periodical time-varying cavity length will induce periodic phase change of the delayed versions when the cavity length of the filter is modulated by a small AC dithering signal. By this means, we can obtain the dynamic frequency response of the FFP tunable filter by an appropriate modification.

## 2.2. Frequency response at the state of cavity length modulated by an AC signal

When the FFP tunable filter is modulated by a small sinusoidal signal  $V = V_c \cos(\omega_c t)$ , where  $\omega_c$  is the angular frequency of the modulated signal,  $V_c$  is the peak-to-peak value of the AC signal, it will cause a periodical dither on the cavity length. The small periodical time-varying cavity length is

$$d(t) = d_0 + \Delta d_c \sin(\omega_c t) \quad (5)$$

where  $\Delta d_c$  is the maximum variable length, generally, it satisfies  $\Delta d_c \ll d_0$  and is determined by the peak-to-peak value of the modulated signal and the dynamic sensitivity near a certain bias voltage of the FFP tunable filter. Based on a reasonable simplifying assumption, the static sensitivity can be substituted for the dynamic sensitivity. And then the maximum variable length can be calculated according to the relationship between the cavity length and the static sensitivity,  $\Delta d_c = V_c \lambda / 2V_{\text{FSR}}$ , where  $V_{\text{FSR}}$  is the voltage driven on the PZT of the tunable filter and the variation of the cavity length is  $\lambda/2$ . In other words, the shift of the resonant frequency is a FSR. Then the instantaneous angular frequency of the FFP tunable filter  $\omega_A = \omega + \rho \sin(\omega_c t)$ , where  $\rho$  is the maximum angular frequency deviation, which is given by  $\rho = \pi c V_c / d_0 V_{\text{FSR}}$ . Then the frequency response of the FFP filter at the state of the cavity length modulated by an AC signal can be obtained

$$H(\omega_A) = \sum_{n=0}^{\infty} a_n \exp\left[-j(\omega + \rho \sin(\omega_c t))n\tau\right] \quad (6)$$

This analytical expression is robust and simple for computer calculation, and the dynamic time response of a FFP tunable filter modulated by an AC signal can be easily obtained from this dynamic frequency response.

### 2.3. Time response at the state of cavity length modulated by an AC signal

In practice, the locking stability of a FFP tunable filter is usually observed and measured through its time domain response, Eq. (3) can be expressed as the exponential form,

$$H(\omega) = \frac{T}{1 - \eta R \exp(-j\omega\tau)} \quad (7)$$

Further, assuming  $\Delta\omega$  and  $\omega_{\text{FSR}} = 2\pi\Omega_F$  are the full width at half maximum (FWHM) and the FSR in angular frequency domain, respectively, this frequency response of the FFP tunable filter can be transformed into a form independent of the time factor;  $\omega_q = q\omega_{\text{FSR}}$  is the resonance frequency with the  $q$ -th longitudinal mode of the filter, it satisfies  $\exp(-j\omega_q\tau) = 1$ . When the frequency of incident beam  $\omega$  is near the resonance,

$$\exp(-j\omega\tau) = \exp\left(-\frac{j\omega}{\Omega_F}\right) \approx 1 - \frac{j(\omega - \omega_q)}{\Omega_F} \quad (8)$$

Equation (7) is rewritten near the resonance frequency as

$$H(\omega) = \frac{1}{1 + 2i(\omega - \omega_q)/\Delta\omega} \quad (9)$$

where  $(\omega - \omega_q) \ll \Delta\omega$  is satisfied, the higher order terms of  $(\omega - \omega_q)/\Delta\omega$  are neglected and the efficiency factor  $\eta$  is regarded as 1.

The time response of the FFP tunable filter at the state of cavity length modulated by an AC signal is given as

$$T(\omega, t) = \frac{1}{1 + 2i[\alpha + \beta \sin(\omega_c t)]} \quad (10)$$

where  $\alpha = (\omega - \omega_q)/\Delta\omega$ , and  $\beta = \rho/\Delta\omega$ .

We defined  $\alpha$  as the relative misadjustment of the incident frequency and the resonance frequency,  $\beta$  is the modulation width which is related to the maximum angular frequency deviation  $\rho$  and FWHM of the filter. For a single frequency laser with the intensity  $I_0$ , the detected voltage of a photodetector (PD) at the filter output is

$$V_D = I_0^2 |T(\omega, t)|^2 \quad (11)$$

When a FFP tunable filter is modulated by an AC signal, this time the response can be utilized to evaluate and calculate the relative maladjustment between the central wavelengths of the filter and the laser. Next, we will simulate the static characteristics and dynamic behaviors. Experimental results will provide further demonstrations for the effects of the amplitude and frequency of the AC dithering signal on locking stability.

### 3. Numerical simulation and analysis

Assuming that the cavity length  $d_0$  of a FFP tunable filter at a certain bias voltage is 1.1 mm, the reflectivities of the mirrors are all 0.9 and the efficiency factor is 1, the wavelength (frequency) response can be simulated simply according to the signal processing method. The magnitude frequency response  $H(\omega)$  of the FFP filter is shown in Fig. 2. It can be seen that the comb spectral characteristics is identical with the classical Airy function.

The phase frequency (wavelength) characteristics indicates the difference between the phase of the transmission output and the phase of the incident beam. For a longitudinal mode, Fig. 2 shows that the phase difference is opposite when the incident wavelength is located symmetrically at different side of the resonant peak point nearby. These indicate that the two symmetric sidebands of a phase modulated light exists the  $\pi$ -phase difference while passing through the filter and beating with the optical carrier at the PD in Ref. [1].

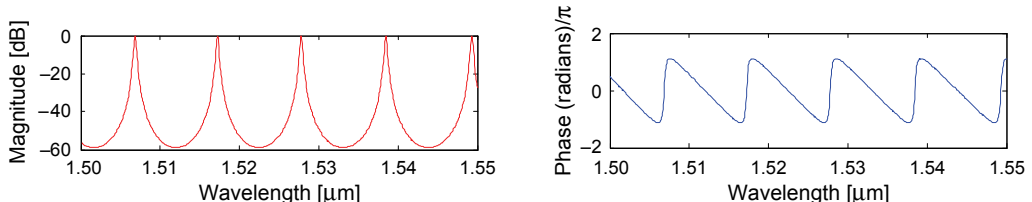


Fig. 2. Wavelength characteristics of FFP tunable filter at the state of fixed cavity length.

When the FFP tunable filter is modulated by an AC dither signal, the dynamic response is simulated and shown in Fig. 3, where the wavelength range is selected from 1554 to 1555.6 nm. The curves are all the superposition of the multiple sub-carriers generated by the AC modulation signal and the frequency response  $H(\omega)$  at the state of fixed cavity length. The wavelength interval between the sub-carriers tends to decrease with the increasing frequency in Fig. 3a. Figure 3b shows that the amplitude of each sub-carrier increases with the increasing maximum angler frequency deviation  $\rho$ . These show that large amplitude rather than large frequency of the AC signal can destroy the quasi-static resonance in the transmitted spectrum of the FP cavity. According to the demand of the dithering technique, the maximum angler frequency deviation can be selected as no more than  $\rho = 0.005c/d_0$  from Fig. 3b.

Figure 4a illustrates the time response at the state of cavity length modulated by an AC signal in the cases of  $\alpha = 0$ . It can be seen that one cycle of the dither signal produces a detected signal at a frequency which is twice as the dither frequency. When the value of  $\beta$  is relatively small ( $\beta = 0.2, 0.7$ ), the detected signal is weaker. However,

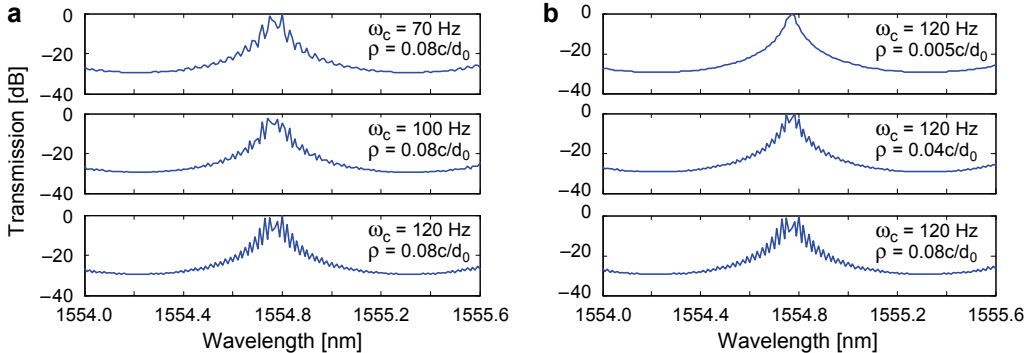


Fig. 3. Simulated magnitude-wavelength (frequency) response of FFP tunable filter modulated by an AC dithering signal. Different modulation angular frequency (a), and different maximum angular frequency deviation (b).

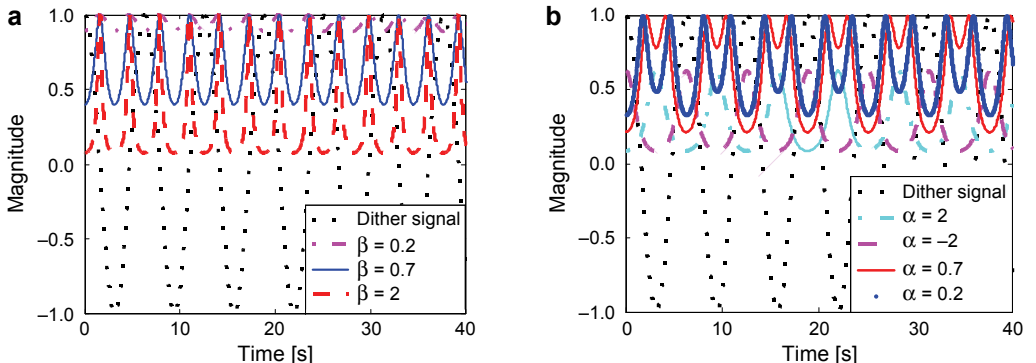


Fig. 4. Simulated time domain response of PD signal at the situation of no relative maladjustment  $\alpha = 0$  (a), and near zero relative maladjustment (b).

the waveform of the detect signal will show a serious distortion when the value of  $\beta$  is relatively stronger ( $\beta = 2$ ). Therefore, by judging the appearance of twice the dither frequency of the detected signal, we can determine whether the central wavelength of the filter is locked at the central wavelength of the laser. Meanwhile, the distortion with the stronger value  $\beta$  further shows that the amplitude of the AC signal should not be selected as too large.

The case of the detected signal near  $\alpha = 0$  is shown in Fig. 4b. When the relative misadjustment of the laser frequency and the filter frequency is relatively smaller ( $\alpha = 0.2, 0.7$ ), the curve of the detected signal exhibits an approximated saddle-shaped analogy to the Lamb dip [13]. The phenomenon of a smaller saddle point and narrow dip indicates a smaller relative maladjustment. When the value of  $\alpha$  is relatively stronger ( $\alpha = 2, -2$ ), the curve of the detected signal exhibits a signal peak. It shows that the phase of the detected signal is the same as that of the dither signal when  $\alpha$  is positive, and the phase difference between the detected signal and the dither signal is  $\pi$  when  $\alpha$  is negative. These simulation results can be utilized to calculate the relative maladjustment between the central wavelength of the filter and the laser.

## 4. Experiment results

The experiment setup used to measure the locking stability of a FFP tunable filter and evaluate the parameters of the dithering signal is shown in Fig. 5. The source is a single-wavelength DFB laser diode with a center wavelength of 1551.37 nm. The FSR of the FFP tunable filter is 1.1 nm and its finesse is 12 at the test wavelength 1550 nm. Light from the DFB source is filtered by the filter and then divided into two beams by an optical coupler. One beam is detected by a PD for oscilloscope (OSC), and the other beam is sent to the optical spectrum analyzer (OSA).

Firstly, a bias voltage is applied to tune the filter to the maximum transmittance. Then a sinusoidal dither signal is additionally driven on the filter (Fig. 6a). The wavelength intervals between the sub-carriers are 0.026, 0.014 and 0.017 nm when the mod-

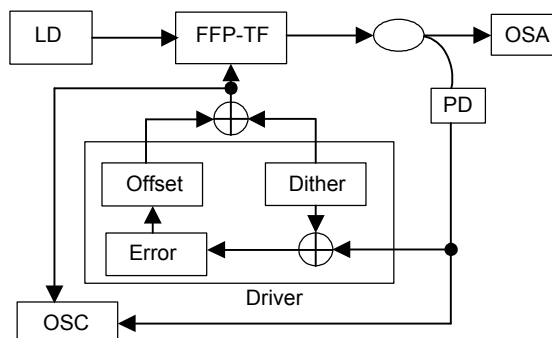


Fig. 5. Experimental setup used to measure the locking stability and evaluate the parameters of dithering signal. LD – laser diode, FFP-TF – fiber Fabry-Pérot tunable filter, OSA – optical spectrum analyzer, PD – photodetector, OSC – oscilloscope.

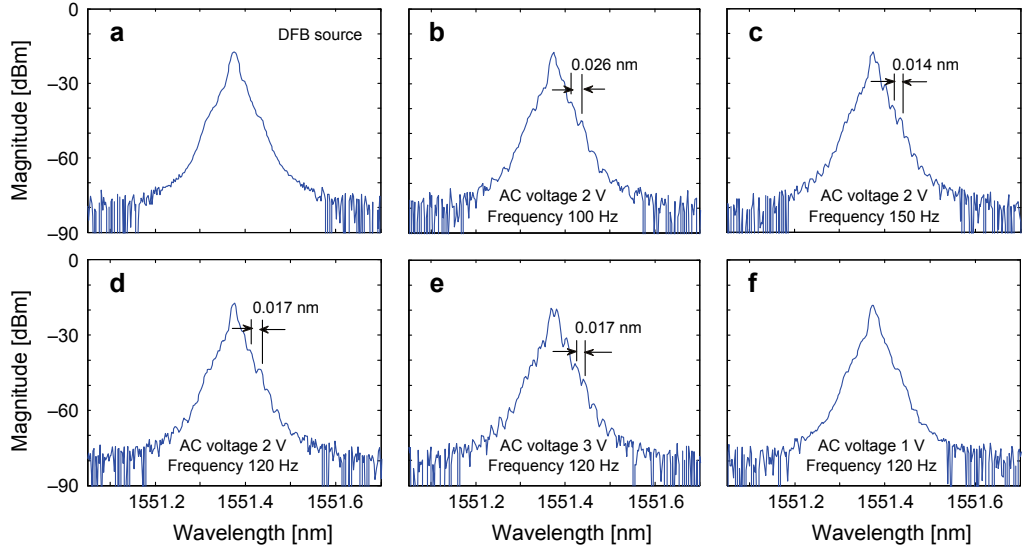


Fig. 6. Measured magnitude-wavelength (frequency) response of FFP tunable filter modulated by different frequency and different amplitude. (See text for explanation.)

ulation frequency is 100, 150 and 120 Hz, respectively, in Figs. 6b–6d. Figs. 6d–6f show that the wavelength intervals between the sub-carriers are all 0.017 nm for the AC voltage 1, 2 and 3 V, respectively, (the intensity of the sub-carrier is weak at 1 V). The results show that the maximum amplitude should be selected as no more than 1 V according to the demand of quasi-static resonance.

When the frequency of the low pass filter after the PD is designed as 10 kHz, a small sinusoidal signal, selected with the amplitude of 1 V and frequency of 1.4 kHz,

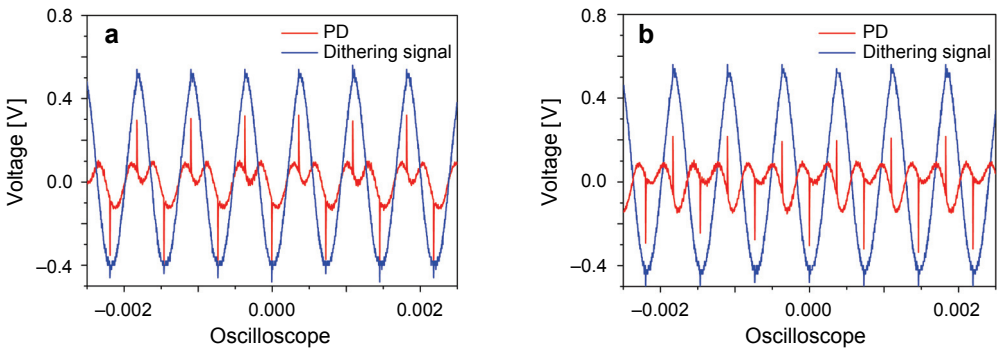
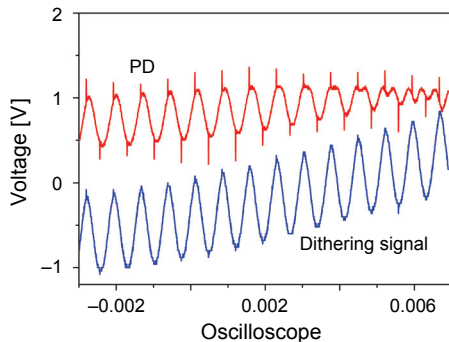


Fig. 7. Measured signals from the photodetector when the filter is modulated by an AC dither signal. Measured operation process of FFP tunable filter for the wavelength tracking and locking. The laser center wavelength is inboard of the center of filter passband (**a**); the laser center wavelength is outboard of the center of filter passband (**b**).



► Fig. 8. Measured operation process of FFP tunable filter for the wavelength tracking and locking.

is applied to drive the filter for realizing wavelength tracking and locking of the DFB laser diode. A special electric circuit is designed to display the phase delay of the detected signal caused by the PZT. The time response is shown in Fig. 7. The detected signal at a frequency twice as the dither frequency is shown in Figs. 7a and 7b, respectively. It clearly shows that the selected frequency and magnitude of the dithering signal can satisfy the demand of a control circuit. In addition, the detected signal is either in phase or out of phase with the dither signal, which depends upon whether the laser center wavelength is inboard or outboard of the center of a filter passband. These are decided by the character of a phase-wavelength response of the FFP tunable filter in Fig. 2.

To lock the central wavelength of the filter at the central wavelength of the laser, the detected signal needs to be mixed with a reference dithering signal in a phase-lock-loop (PLL) circuit. The PLL output is either a positive or a negative DC signal, which is amplified and used to adjust the bias current driven on the filter. Then the FFP tunable filter can be tuned by the polarity of the PLL output towards a point of maximum transmission for tracking the central wavelength of the laser. The measured operation process of the FFP tunable filter for the wavelength tracking and locking is shown in Fig. 8. It can be seen that the mean voltage of the dither signal is adjusted by the PLL output signal, and an approximated double peak.

## 5. Conclusions

We have proposed a signal processing method to model the dynamic responses of a FFP tunable filter with the dithering control technique. Based on the static analysis of the FFP filter at the state of fixed cavity length, the dynamic frequency response is obtained by modification of the static transfer function of the device for the case of cavity length modulated by a dithering signal. Static characteristics and dynamic behaviors are also investigated. Effects of amplitude and frequency of the AC dithering signal on locking stability can be observed from simulation results, either from the frequency responses or the time response. Experimental results also imply the dependence

of the locking stability of a FFP tunable filter on the amplitude of a dithering signal, which matches well with the theoretical simulation.

*Acknowledgements* – This work was supported in part by the National Natural Science Foundation of China under Grant No. 60677024 and the National High Technology Research Development Program of China under Grant No. 2009AA03Z418.

## References

- [1] YUBIN JI, SHILIE ZHENG, ZE LI, XIAOFENG JIN, XIANMIN ZHANG, HAO CHI, *Tunable fiber Fabry–Perot filter for PM–IM conversion and efficiency improvement in radio-over-fiber links*, *Microwave and Optical Technology Letters* **52**(9), 2010, pp. 2090–2095.
- [2] TARANENKO N.L., TENBRINK S.C., HSU K., MILLER C.M., *Fiber Fabry–Perot tunable filter for high-speed optical packet switching*, *Proceedings of SPIE* **2918**, 1997, pp. 26–37.
- [3] YI JIANG, *Fourier transform white-light interferometry for the measurement of fiber-optic extrinsic Fabry–Perot interferometric sensors*, *IEEE Photonics Technology Letters* **20**(2), 2008, pp. 75–77.
- [4] DECUSATIS C., JACOBOWITZ L., *Wavelength locked loops for optical communication networks*, *Proc. IEEE Sarnoff Symposium*, Session S13, Princeton, N.J., 2007, pp. 48–52.
- [5] KERSEY A.D., BERKOFF T.A., MOREY W.W., *Multiplexed fiber Bragg grating strain-sensor system with a fiber Fabry–Perot wavelength filter*, *Optics Letters* **18**(16), 1993, pp. 1370–1372.
- [6] PARK P.K. J., CHUNG Y.C., *Analysis of frequency offset in the frequency stabilization of semiconductor laser based on frequency dithering technique*, *Optics Express* **15**(21), 2007, pp. 14213–14218.
- [7] BONDU F., DEBIEU O., *Accurate measurement method of Fabry–Perot cavity parameters via optical transfer function*, *Applied Optics* **46**(14), 2007, pp. 2611–2614.
- [8] LOCKE C.R., STUART D., IVANOV E.N., LUTTEN A.N., *A simple technique for accurate and complete characterisation of a Fabry–Perot cavity*, *Optics Express* **17**(24), 2009, pp. 21935–21943.
- [9] NAKAZAWA M., *Phase-sensitive detection on Lorentzian line shape and its application to frequency stabilization of lasers*, *Journal of Applied Physics* **59**(7), 1986, pp. 2297–2305.
- [10] LAWRENCE M.J., WILLKE B., HUSMAN M.E., GUSTAFSON E.K., BYER R.L., *Dynamic response of a Fabry–Perot interferometer*, *Journal of the Optical Society of America B* **16**(4), 1999, pp. 523–532.
- [11] RAKHMANOV M., SAVAGE R.L. JR., REITZE D.H., TANNER D.B., *Dynamic resonance of light in Fabry–Perot cavities*, *Physics Letters A* **305**(5), 2002, pp. 239–244.
- [12] MADSEN C.K., ZHAO J.H., *Optical Filter Design and Analysis – A Signal Processing Approach*, Wiley, 1999, pp. 96–106.
- [13] BORRI S., BARTALINI S., GALLI I., CANCIO P., GIUSFREDI G., MAZZOTTI D., CASTRILLO A., GIANFRANI L., DE NATALE P., *Lamb-dip-locked quantum cascade laser for comb-referenced IR absolute frequency measurements*, *Optics Express* **16**(15), 2008, pp. 11637–11646.

Received May 31, 2011